He contributions to the SPI $\Delta\sigma_y$

Figure 4 shows the isolated He hardening σ_{He} decomposed based on Eq.(2) super-positioning for SPI irradiated F82H and Eurofer97 alloys [13-19] as a function of √He (appm$^{1/2}$) for T_i 100°C groups. Due to large uncertainties and lack of relevance, the data for $T_i < \approx$ 100°C and 9Cr1Mo alloys were excluded. The general softening trends shown in Figure 3c is used for $\Delta\sigma_{y,N}$(dpa, T_i, T_t) for $T_i = T_t >$ 450°C. Note, high He SPI $\Delta\sigma_y$ data are also limited by linear elastic fracture. The elastic tensile fracture data indicate a large reduction of intergranular fracture stress, which will be used in fracture models to be reported in the future. Figure 4 also includes an isolated He hardening decomposed for microstructure observed in ISHI irradiated Eurofer97 at 500°C to 21.2 dpa and 1230 appm He [20]. Obtained σ_{He} - √He trends are similar for F82H and Eurofer97, so the combined trends are that $\sigma_{He} \approx 0$ at He $< \approx$ 433 appm, then increase ≈ linearly with √He as:

$$\sigma_{He} = 28.4\ (\sqrt{He}-20.8) \qquad (8)$$

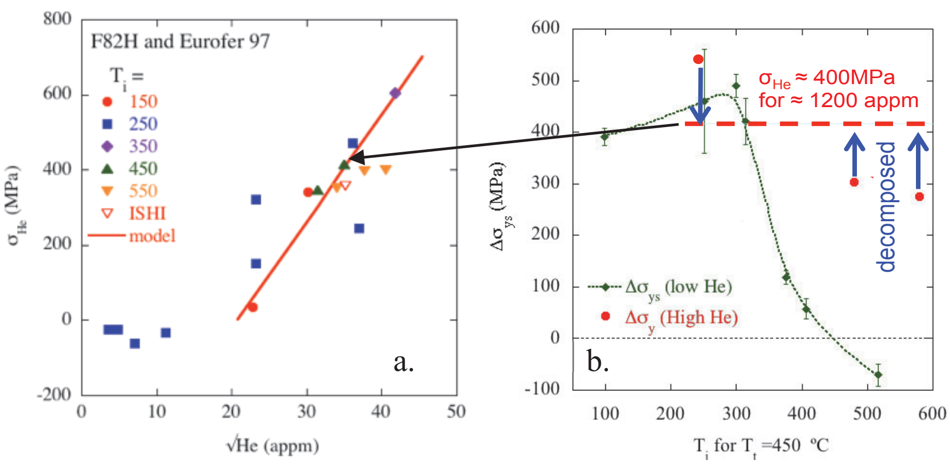

Figure 4 a) Isolated He hardening σ_{He} for SPI irradiated F82H and Eurofer97 alloys shown for T_i groups with overall fitting for He > 500. Open triangle is for a hardening estimated for the microstructure observed in ISHI irradiated Eurofer97 at 500°C to 21.2 dpa and 1230 appm He; b) examples of decomposed σ_{He} from SPI $\Delta\sigma_y$ at various T_i in relation to low He $\Delta\sigma_y$(T) trend.

Combining σ_{He}(He) in Eq(8) with the neutron only $\Delta\sigma_{y,N}$(dpa, T_i, T_i) models can generate $\Delta\sigma_y$ prediction models for various He/dpa cases. For example, Figure 5 shows a model for F82H at He/dpa = 80, corresponding to a typical SPI condition at Ti = 300 to 500°C. SPI measured $\Delta\sigma_y$, plotted along are in good agreement with the models.

High He effects on flow stress changes

The uniform engineering strains in tensile tests on neutron irradiated TMS (and other metals and alloys) are typically < 1%, due to plastic instabilities and immediate necking. However, in SPI steels, with high He, uniform-engineering strains are typically several percent (necking is delayed). Figure 6a shows true stress-strain curves [3,14-15], $\sigma(\varepsilon)$, used to estimate true flow stress changes. The unirradiated $\sigma(\varepsilon)$ shows typical strain hardening. The NI $\sigma(\varepsilon)$ shows slight initial softening. The $\sigma(\varepsilon)$ with high He concentration do not show immediate drop after yielding suppressing loss of strain hardening, which is generally observed after neutron only irradiation. The effects result in gradual but continuous increase in $\Delta\sigma_{fl}$ to $\Delta\sigma_y$ ratio as shown in Figure 6b. This will lead a larger transition temperature shift in fracture toughness, since $\Delta\sigma_{fl}$ is more directly correlated to ΔT_o[4]. It is notable that the total elongation decreases a lot – may be IG fracture occurs after a little strain hardening.